182476: migmatitic gneiss, Big Red prospect

(Recherche Supersuite, Albany–Fraser Orogen)

Location and sampling

SEEMORE (SH 51-12), CLAYPAN (3837)
MGA Zone 51, 688400E 6649200N

Sampled on 17 August 2010

This sample was collected from diamond drillcore from hole BRDDH002, located on the Big Red prospect, at a depth of 114.6 – 115.6 m. The hole was drilled by Teck Australia Pty Ltd, and was co-funded through the Exploration Incentive Scheme. The drillhole is located on the Nullarbor Plain, approximately 16.4 km south of Fifty Mile Claypan, 36.2 km northeast of Native Willow Bore (Kananda Station), and 57.5 km west of radio mast R204 on the Rawlinna–Warburton Road (Connie Sue Highway).

Tectonic unit/relations

The sample is from drillhole BRDDH002, which penetrated Precambrian basement rocks beneath the Mesozoic–Cenozoic Eucla Basin at a depth of 102.2 m; the total depth of the hole was 147.6 m. BRDDH002 was drilled to investigate a subcircular gravity high, located approximately 2 km west of a magnetic high interpreted from detailed aeromagnetic data as a potential magnetite-bearing stratigraphic iron-formation, possibly associated with copper–gold mineralization (Tillick, 2010). This magnetic anomaly is located within the eastern Nornalup Zone of the Albany–Fraser Orogen, which contains 1800–1760 Ma metagranitic rocks similar in age to some metagranitic rocks in the Biranup Zone, overlain by metasedimentary rocks of the Arid Basin (Spaggiari et al., 2011). The Nornalup Zone is intruded by rocks of the Mesoproterozoic Recherche and Esperance Supersuites (Nelson et al., 1995).

The Precambrian rocks in BRDDH002 comprise strongly deformed and metamorphosed rocks, including foliated, garnet-bearing amphibolite and mafic granulite (up to 5 m thick); coarse-grained K-feldspar–quartz–biotite granitic gneiss, of which the present sample is representative; and folded, garnet-bearing psammitic gneiss (see also Tillick, 2010). These rocks represent a succession of migmatitic paragneissic and metagranitic rocks, with possible mafic sills. A sample of mafic granulite (GSWA 182477, Kirkland et al., 2012d) from this same drillhole yielded an age of metamorphism of 1188 ± 4 Ma.

Three additional samples at the Big Red prospect were dated from drillhole BRDDH001, located 2.1 km to the east of BRDDH002. Two samples of migmatitic gneiss (GSWA 182473, Kirkland et al., 2012a; GSWA 182475, Kirkland et al., 2012c) yielded maximum depositional ages (1σ) of 1729 ± 27 and 1685 ± 11 Ma, respectively. These rocks are intruded by veins of granite pegmatite, one of which (GSWA 182474, Kirkland et al., 2012b) provided a crystallization age of 1167 ± 2 Ma.

Petrographic description

The sample is a migmatitic gneiss composed of 50% quartz, 35% feldspar, 10% biotite and amphibole, 4% opaque oxide minerals, and minor chlorite, muscovite, apatite, and zircon. Paleosome bands consist of aggregates of fine- to medium-grained, anhedral, clouded, partly sericite-altered, feldspar. Quartz occurs mainly in leucosome and neosome bands and lenses, which are injected into paleosomes. Feldspars include albite-twinned crystals of albite–oligoclase composition (up to An26) and perthitic K-feldspar. Leucosome bands consist of elongated, coarse-grained quartz mosaics accompanied by minor feldspar. Fine-grained brown biotite flakes and fine- to medium-grained green pleochroic amphibole are commonly concentrated in distinct bands, and are accompanied by granular iron-oxide minerals. Amphibole is crosscut by quartz veins. Minor muscovite flakes are associated with sericite-altered feldspar. Anhedral to subhedral fine-grained apatite is common throughout the sample.

Zircon morphology

Zircons isolated from this sample are subhedral to euhedral, and colourless to dark brown. The crystals are up to 450 μm long, and are elongate, with aspect ratios up to 5:1. In cathodoluminescence (CL) images, most zircons exhibit idiomorphic zoning, and many are variably overgrown and/or transected by homogeneous, high-uranium zircon. A CL image of representative zircons is shown in Figure 1.

Analytical details

This sample was analysed on 7–8 June 2011, using

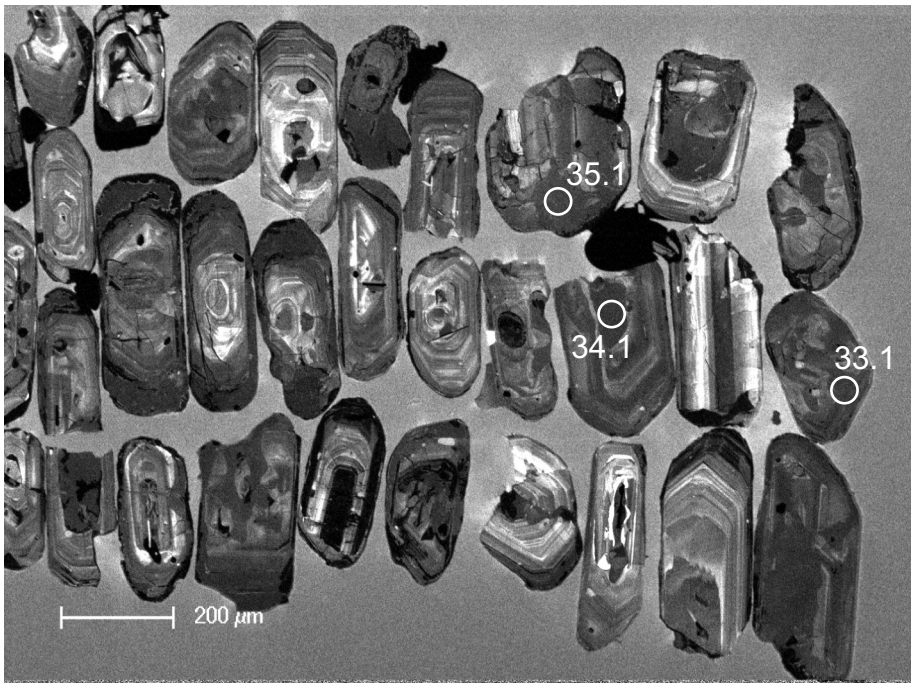

Figure 1. Cathodoluminescence image of representative zircons from sample 182476: migmatitic gneiss, Big Red prospect. Numbered circles indicate the approximate positions of analysis sites.

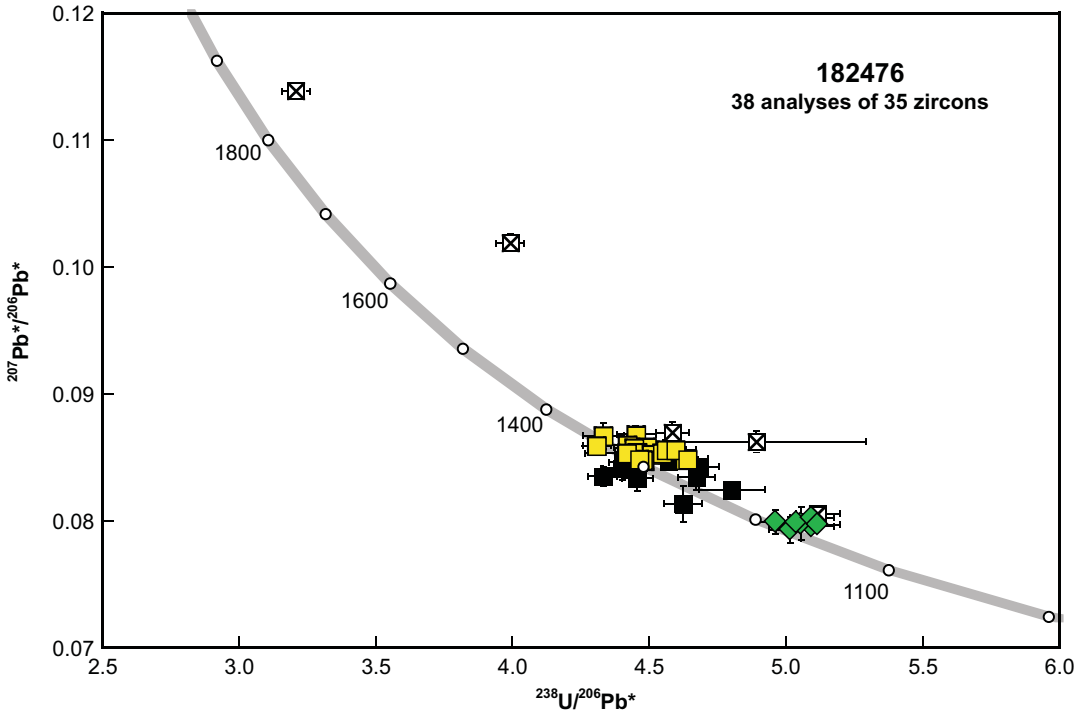

Figure 2. U–Pb analytical data for sample 182476: migmatitic gneiss, Big Red prospect. Yellow squares indicate Group I (magmatic zircons); black squares indicate Group P (radiogenic-Pb loss); green diamonds indicate Group M (metamorphic zircons); crossed squares indicate Group D (discordance >5%).

Table 1. Ion microprobe analytical results for zircons from sample 182476: migmatitic gneiss, Big Red prospect

Group ID	Spot no.	Grain. spot	^{238}U (ppm)	^{232}Th (ppm)	$\frac{^{232}Th}{^{238}U}$	f204 (%)	$^{238}U/^{206}Pb$ ± 1σ		$^{207}Pb/^{206}Pb$ ± 1σ		$^{238}U/^{206}Pb^*$ ± 1σ		$^{207}Pb^*/^{206}Pb^*$ ± 1σ		$^{238}U/^{206}Pb^*$ date (Ma) ±1σ		$^{207}Pb^*/^{206}Pb^*$ date (Ma) ±1σ		Disc. (%)
I	30	27.1	231	248	1.11	0.094	4.477	0.076	0.08549	0.00065	4.481	0.076	0.08470	0.00074	1298	20	1309	17	0.8
I	7	3.2	644	380	0.61	0.061	4.626	0.048	0.08534	0.00037	4.629	0.048	0.08482	0.00040	1261	12	1311	9	3.8
I	24	21.1	322	267	0.86	-0.012	4.638	0.076	0.08474	0.00052	4.637	0.076	0.08485	0.00053	1259	19	1312	12	4.1
I	16	13.1	371	179	0.50	0.058	4.459	0.072	0.08536	0.00051	4.462	0.073	0.08487	0.00056	1304	19	1312	13	0.7
I	31	28.1	285	119	0.43	0.058	4.472	0.074	0.08532	0.00057	4.475	0.074	0.08482	0.00062	1300	20	1312	14	0.9
I	18	15.1	224	200	0.92	-0.018	4.506	0.076	0.08509	0.00065	4.505	0.076	0.08525	0.00066	1292	20	1321	15	2.2
I	9	1.2	861	407	0.49	0.013	4.545	0.047	0.08548	0.00031	4.545	0.047	0.08537	0.00032	1282	12	1324	7	3.2
I	8	7.1	184	253	1.42	0.099	4.413	0.152	0.08621	0.00067	4.417	0.153	0.08536	0.00077	1316	42	1324	17	0.6
I	22	19.1	135	150	1.14	0.118	4.451	0.080	0.08644	0.00082	4.456	0.080	0.08543	0.00096	1305	22	1325	22	1.5
I	19	16.1	289	236	0.85	0.188	4.551	0.076	0.08720	0.00063	4.560	0.076	0.08560	0.00079	1278	20	1329	18	3.8
I	28	25.1	478	199	0.43	-0.060	4.597	0.074	0.08513	0.00044	4.595	0.074	0.08564	0.00048	1269	19	1330	11	4.6
I	26	23.1	408	266	0.67	-0.058	4.446	0.072	0.08526	0.00047	4.444	0.072	0.08576	0.00051	1308	19	1333	11	1.8
I	17	14.1	610	430	0.73	-0.062	4.493	0.071	0.08528	0.00039	4.490	0.071	0.08581	0.00043	1296	19	1334	10	2.8
I	10	5.1	176	98	0.57	-0.039	4.310	0.053	0.08559	0.00067	4.308	0.053	0.08592	0.00071	1346	15	1336	16	-0.7
I	11	3.1	145	71	0.51	-0.027	4.420	0.058	0.08575	0.00078	4.419	0.058	0.08599	0.00082	1315	16	1338	18	1.7
I	20	17.1	156	220	1.45	-0.218	4.341	0.077	0.08485	0.00079	4.331	0.077	0.08671	0.00103	1339	22	1354	23	1.1
I	23	20.1	378	215	0.59	-0.105	4.456	0.072	0.08594	0.00050	4.451	0.072	0.08684	0.00058	1307	19	1357	13	3.7
P	1	8.1	99	146	1.53	0.319	4.609	0.071	0.08405	0.00100	4.624	0.071	0.08134	0.00143	1262	18	1230	35	-2.6
P	2	2.2	866	248	0.30	0.043	4.800	0.121	0.08282	0.00030	4.802	0.121	0.08246	0.00032	1220	29	1256	8	2.9
P	3	1.1	166	182	1.13	0.185	4.448	0.057	0.08491	0.00072	4.456	0.057	0.08334	0.00091	1305	15	1277	21	-2.2
P	4	11.1	141	187	1.38	0.040	4.671	0.069	0.08378	0.00093	4.672	0.069	0.08344	0.00099	1250	17	1279	23	2.3
P	5	6.1	195	192	1.02	0.114	4.325	0.053	0.08448	0.00065	4.330	0.053	0.08351	0.00076	1340	15	1281	18	-4.6
P	25	22.1	140	155	1.14	0.059	4.398	0.078	0.08465	0.00081	4.401	0.078	0.08414	0.00089	1320	22	1296	21	-1.9
P	33	30.1	727	292	0.41	0.020	4.680	0.073	0.08444	0.00033	4.681	0.073	0.08427	0.00034	1248	18	1299	8	3.9
P	6	4.1	186	260	1.44	0.036	4.401	0.054	0.08493	0.00064	4.403	0.054	0.08462	0.00067	1319	15	1307	15	-1.0
P	27	24.1	415	288	0.72	0.070	4.568	0.074	0.08528	0.00047	4.571	0.074	0.08468	0.00053	1275	19	1308	12	2.5
M	32	29.1	1546	51	0.03	0.014	5.015	0.078	0.07944	0.00105	5.016	0.078	0.07932	0.00106	1172	17	1180	26	0.7
M	37	34.1	891	9	0.01	-0.005	5.095	0.080	0.07952	0.00032	5.095	0.080	0.07956	0.00032	1155	17	1186	8	2.6
M	29	26.1	1110	11	0.01	0.061	5.114	0.080	0.08026	0.00030	5.117	0.080	0.07974	0.00033	1151	17	1191	8	3.4
M	38	35.1	1163	15	0.01	-0.052	5.057	0.079	0.07935	0.00130	5.054	0.079	0.07978	0.00130	1164	17	1192	32	2.3
M	15	12.1	2050	147	0.07	-0.012	5.038	0.078	0.07980	0.00022	5.037	0.078	0.07990	0.00023	1167	17	1195	6	2.3
M	34	31.1	1697	44	0.03	0.010	4.962	0.077	0.08001	0.00095	4.962	0.077	0.07993	0.00095	1183	17	1195	23	1.0
M	35	32.1	867	5	0.01	-0.005	5.094	0.080	0.08018	0.00033	5.094	0.080	0.08023	0.00033	1155	17	1203	8	3.9
D	36	33.1	1014	9	0.01	-0.061	5.120	0.080	0.08007	0.00031	5.117	0.080	0.08058	0.00034	1151	17	1211	8	5.0
D	12	9.1	151	199	1.36	0.000	4.891	0.400	0.08625	0.00085	4.891	0.400	0.08625	0.00085	1199	97	1344	19	10.8
D	13	10.1	173	98	0.58	0.027	4.584	0.060	0.08722	0.00079	4.585	0.060	0.08698	0.00083	1272	15	1360	18	6.5
D	14	2.1	247	238	1.00	0.132	3.986	0.049	0.10305	0.00063	3.991	0.049	0.10190	0.00072	1441	16	1659	13	13.1
D	21	18.1	594	6	0.01	-0.024	3.209	0.051	0.11364	0.00041	3.208	0.051	0.11385	0.00042	1749	25	1862	7	6.0

SHRIMP-B, and on 21–22 June 2011, using SHRIMP-A. Analyses 1.1 to 11.1 (spot numbers 1–14) were obtained during the first session, together with 13 analyses of the BR266 standard, which indicated an external spot-to-spot (reproducibility) uncertainty of 0.87% (1σ) and a $^{238}U/^{206}Pb*$ calibration uncertainty of 0.39% (1σ). Analyses 12.1 to 35.1 (spot numbers 15–38) were obtained during the second session, together with 13 analyses of the BR266 standard, of which nine indicated an external spot-to-spot (reproducibility) uncertainty of 1.43% (1σ) and a $^{238}U/^{206}Pb*$ calibration uncertainty of 0.49% (1σ). Calibration uncertainties are included in the errors of $^{238}U/^{206}Pb*$ ratios and dates listed in Table 1. Common-Pb corrections were applied to all analyses using contemporaneous isotopic compositions determined according to the model of Stacey and Kramers (1975).

Results

Thirty-eight analyses were obtained from 35 zircons. Results are listed in Table 1, and are shown in a concordia diagram (Fig. 2).

Interpretation

The analyses are concordant to moderately discordant (Fig. 2). Five analyses are >5% discordant. The dates obtained from these five analyses (Group D; Table 1) are imprecise or unreliable, and are considered not geologically significant. The remaining 33 analyses can be divided into three groups, based on their $^{207}Pb*/^{206}Pb*$ ratios and analytical positions within the crystals.

Group I comprises 17 analysis of 17 zircon cores (Table 1), which yield a weighted mean $^{207}Pb*/^{206}Pb*$ date of 1326 ± 6 Ma (MSWD = 1.04).

Group P comprises nine analyses of nine zircon cores (Table 1), which yield $^{207}Pb*/^{206}Pb*$ dates of 1308–1230 Ma.

Group M comprises seven analyses of seven zircon rims or homogeneous domains (Table 1), which yield a concordia age of 1187 ± 9 Ma (MSWD = 1.7).

The date of 1326 ± 6 Ma for the 17 analyses in Group I is interpreted as the magmatic crystallization age of the granitic protolith. This age is consistent with the granite belonging to the Recherche Supersuite (Nelson et al., 1995). The dates of 1308–1230 Ma for the nine analyses in Group P are interpreted to reflect minor ancient radiogenic-Pb loss.

The date of 1187 ± 9 Ma for the seven analyses in Group M is interpreted as the age of a high-grade metamorphic event during Stage II (1215–1140 Ma) of the Albany–Fraser Orogeny (Clark et al., 2000).

References

Clark, DJ, Hensen, BJ and Kinny, PD 2000, Geochronological constraints for a two-stage history of the Albany–Fraser Orogen, Western Australia: Precambrian Research, v. 102, no. 3, p. 155–183.

Kirkland, CL, Wingate, MTD and Spaggiari, CV 2012a, 182473: migmatitic gneiss, Big Red prospect; Geochronology Record 1050: Geological Survey of Western Australia, 6p.

Kirkland, CL, Wingate, MTD and Spaggiari, CV 2012b, 182474: granite vein, Big Red prospect; Geochronology Record 1051: Geological Survey of Western Australia, 4p.

Kirkland, CL, Wingate, MTD and Spaggiari, CV 2012c, 182475: migmatitic gneiss, Big Red prospect; Geochronology Record 1052: Geological Survey of Western Australia, 7p.

Kirkland, CL, Wingate, MTD and Spaggiari, CV 2012d, 182477: mafic granulite, Big Red prospect; Geochronology Record 1055: Geological Survey of Western Australia, 4p.

Nelson, DR, Myers, JS and Nutman, AP 1995, Chronology and evolution of the Middle Proterozoic Albany–Fraser Orogen, Western Australia: Australian Journal of Earth Sciences, v. 42, p. 481–495, DOI:10.1080/08120099508728218.

Spaggiari, CV, Kirkland, CL, Pawley, MJ, Smithies, RH, Wingate, MTD, Doyle, MG, Blenkinsop, TG, Clark, C, Oorschot, CW, Fox, LJ and Savage, J 2011, The geology of the east Albany–Fraser Orogen — a field guide: Geological Survey of Western Australia, Record 2011/23, 98p.

Stacey, JS and Kramers, JD 1975, Approximation of terrestrial lead isotope evolution by a two-stage model: Earth and Planetary Science Letters, v. 26, p. 207–221.

Tillick, D 2010, Final report of co-funded government–industry drilling program at the Eucla Project, E28/1608, September 2010; Teck Australia Pty Ltd: Geological Survey of Western Australia, Statutory mineral exploration report, A88011, 23p. (unpublished).

Recommended reference for this publication

Kirkland, CL, Wingate, MTD and Spaggiari, CV 2012, 182476: migmatitic gneiss, Big Red prospect; Geochronology Record 1053: Geological Survey of Western Australia, 4p.

Data obtained: 22 June 2011

Data released: 30 June 2012